JMEPEG (1993) 2:703-714

An Innovative Strategy for Open Loop Control of Hot Deformation Processes

J.C. Malas, R.D. Irwin, and R.V. Grandhi

A new strategy for systematically calculating near optimal control parameters for hot deformation processes is presented in this article. This approach is based on modern control theory and involves deriving state-space models directly from available material behavior and hot deformation process models. Two basic stages of analysis and optimization are established in this strategy for nonlinear, open loop control system design for producing required microstructural characteristics, uniformity of deformation and temperature distribution, and other important physical requirements of hot worked products.

Keywords

finite element analysis, hot workability, microstructural control, modern control, optimization methods

1. Introduction

THE potential for cost and quality improvements in the manufacture of products is largely dependent on the status of process control technology as implemented on the shop floor. The production of high-quality products on a reproducible basis can be achieved only through the use of automated control systems. Computer-based control and data acquisition systems for metalforming processes are increasingly being incorporated on production equipment. Commands are preprogrammed in the control system for (1) executing specified ram-velocity profiles, (2) achieving final ram displacements, and (3) maintaining desired temperature distributions. Modern metalforming equipment such as servo-hydraulic forge presses and section rolling mills possess the necessary dynamic response characteristics for implementing the process control algorithms mentioned above. However, existing process design methods for optimizing these control system inputs are highly deficient because they are generally *ad hoc* and lack sufficient consideration of workpiece (material) behavior and understanding of process mechanics. This situation presents major challenges to process engineers who are faced with ever increasing constraints on cost and quality, as well as growing production requirements for near-net shape components with controlled microstructures and properties. Indeed, current approaches to control system design and execution of metalforming processes must be improved if the total quality benefits of automation are to be realized.

A new strategy for systematically calculating near optimal control parameters for hot metal deformation processes is presented in this article. This approach is based on modern control theory and involves developing state-space models from available material behavior and hot deformation process models. Two basic stages of analysis and optimization are established in this strategy for control system design. In the first stage, the kinetics of certain dynamic microstructural behavior and the intrinsic hot workability of the metal/alloy system are used, together with an appropriately chosen optimality criterion, to calculate strain, strain rate, and temperature trajectories. These trajectories are process independent in the sense that they are valid for different hot deformation processes such as forging, extrusion, and rolling and are thus independent of die geometry and flow pattern. A high-fidelity finite-element simulation of the particular process of interest is then used in the second stage to calculate process control parameters such as ram velocity trajectories and billet temperature, which approximately achieve the strain, strain rate, and temperature trajectories calculated in the first stage. The process control parameters are calculated by applying closed loop control principles to the finite-element simulation to maintain the strain, strain rate, and temperature trajectories near those calculated in the first stage.

This article details the rationale used in choosing the optimality criterion used in the first stage of the method and presents a general strategy for systematically finding the optimal trajectories. A significant portion of this article is devoted to detailing the application of closed loop control principles to finite-element process simulations to determine the process control parameters. Included are (1) an explanation of the necessity of the approach, (2) a discussion of the advantages and disadvantages of various control system design techniques, and (3) a detailed discussion of how one particular design technique can be used to calculate process control parameters.

State-space models of deformation processes are necessary to utilize the advanced design capabilities of modern closed loop control techniques. The nonlinear rigid viscoplastic finite-element method is used for deformation and thermal analyses. A finite-element-based condensation technique is used to reduce the number of degrees of freedom of the system. A coupled state-space model is then built to represent the deformation and thermal behavior of the material, with nodal velocities and nodal temperatures as the state variables. The state-space model dynamically changes at every time step for accommodating the evolving workpiece geometry and boundary conditions. The desired microstructural behavior is achieved by controlling effective strain rate and temperature variation within the simulated deforming material. The output variables of the state-space system are effective strain rates and nodal temperatures of critical regions.

J.C. Malas, Materials Directorate, Wright Laboratory, Wright-Patterson AFB, OH, 45433; **R.D. Irwin,** Electrical and Computer Engineering, Ohio University, Athens, OH, 45701; and **R.V. Grandhi,** Mechanical and Materials Engineering, Wright State University, Dayton, OH, 45435.

Symbols

A_D	Condensed plant matrix of deformation process system
A_{DT}	Condensed plant matrix of coupled deformation and thermal system
A_k	Plant matrix at time t_k
A_T	Condensed plant matrix of thermal process system
B_D	Condensed control input matrix of deformation process
B_{DT}	Condensed control input matrix of coupled deformation and thermal system
B_k	Control input matrix at time t_k
C_k	Control output matrix at time t_k
C_T	Heat capacity matrix
F	Load (force) vector of finite-element formulation
J	Optimality criterion
J_{work}	Certain J terms for hot workability properties
J_{micro}	Certain J terms for microstructure development
K	Stiffness matrix of finite-element formulation
K_c	Heat conduction matrix of finite-element formulation
K_k	State variable feedback gain matrix at time t_k
K_S	Secant stiffness matrix
K_T	Tangent stiffness matrix
Q	Matrix weight on state variables
Q_T	Heat flux vector of finite-element formulation
R	Matrix weight on control inputs
T	Hot working temperature
T_{Billet}, T_B	Billet temperature
$T_\sim$	Finite-element prediction of T
T_{TRAJ}	Desired T profile (trajectory)
T_{work}	Nominal T value for acceptable workability
V	Global velocity vector of finite-element formulation
V_{RAM}, V_d	Ram velocity, die velocity
W_D	Constant perturbation vector of deformation model
W_T	Constant perturbation vector of thermal model
x_k	State vector for $t_k \le t < t_{k+1}$
d	Dynamic grain size
g	Cost function over entire trajectory of J
h	Terminal penalty function of J
t	Time
t_f	Final time for complete deformation
t_0	Initial time for start of deformation
u_k	Control input vector $t_k \le t < t_{k+1}$
x	Volume fraction recrystallized
x_f	Specified final x-value
α_1, α_2	Weighting factors for terms of J
β_1, β_2, β_3	Weighting factors for terms of J_{work}
ε	True, plastic strain
$\varepsilon_{0.5}$	Plastic strain for 50 vol% recrystallization
ε_{SIM}	Finite-element prediction of ε
ε_{TRAJ}	Specified ε profile (trajectory)
$\dot{\varepsilon}$	Effective strain rate
$\dot{\varepsilon}_{SIM}$	Finite-element prediction of $\dot{\varepsilon}$
$\dot{\varepsilon}_{TRAJ}$	Specified $\dot{\varepsilon}$ profile (trajectory)
$\dot{\varepsilon}_{work}$	Nominal $\dot{\varepsilon}$ value for acceptable workability

Applications of each of the parts of the two-stage method are presented. In the case of calculating optimal strain, strain rate, and temperature trajectories, phenomenological equations for dynamic recrystallization of plain-carbon steel are used. To illustrate the effectiveness of the second stage, that of calculating process control parameters via closed loop simulation control, a U-section forging of Ti-6242 is presented.

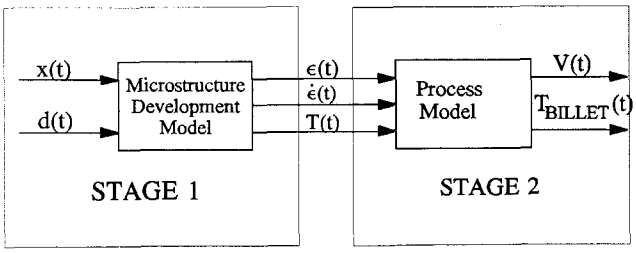

Fig. 1 Block diagram illustrating the two-stage calculation of process control parameters.

2. Two-Stage Approach to Designing Process Parameters

Goals of process control can be met through several different control system design strategies ranging from open loop to sophisticated closed loop control systems. In this work, an optimal control technique[1,2] is used for the design of open loop, nonlinear control of hot metal deformation processes. This modern control method requires three basic characteristics for defining and setting up the control problem: (1) a dynamical system model, (2) physical constraints, and (3) an optimality criterion. In metalforming, the system models of interest are material behavior and deformation process models; constraints include the hot workability of the workpiece and the limitations of the forming equipment. Optimality criteria could be related to achieving a particular final microstructure, regulating temperature, and/or maximizing deformation speeds.

The present two-stage approach decomposes the analysis and optimization into a workpiece material behavior control problem and a process mechanics control problem. As shown in Fig. 1, the material behavior model has control outputs—$\varepsilon(t)$, $\dot{\varepsilon}(t)$, and $T(t)$—which are used in determining the control outputs—$V(t)$, $T_B(t)$—of the process model. Goals of the first stage are to achieve enhanced workability and prescribed microstructural parameters. In the second stage, a primary goal is to achieve the thermomechanical conditions determined from stage one for prescribed regions of the deforming workpiece. It is recognized that this two-stage approach yields idealized process control solutions that could be further improved with advanced feedback methods.

2.1 *Material Behavior and Process Modeling Issues*

The effectiveness of the two-stage approach presented in this article is largely dependent on the availability and reliability of the material behavior and process models to be used. In the first stage, material behavior models that describe the kinetics of primary metallurgical mechanisms such as dynamic recovery, dynamic recrystallization, and grain growth during hot working are required for analysis and optimization of material system dynamics. These mechanisms have been studied extensively for a wide range of metals and alloys.[3-7] The relation-

ships for describing particular microstructural processes have been developed and reported for conventional materials such as aluminum, copper, nickel, and their dilute alloys, with steel receiving the most study. Elsewhere,[8,9] it was claimed that, for certain ranges of temperature and strain rate, the operative deformation mechanisms of specialty alloys such as superalloys, intermetallics, ordered alloys, and metal matrix composites potentially become well defined and are amenable for modeling.

In several industries, process modeling has reached a high level of sophistication and acceptance as a process analysis tool.[10,11] Current process models are capable of analyzing fairly complex material flow operations such as three-dimensional, nonisothermal deformation processes with a sufficiently high degree of accuracy. For example, in the forging industry, detailed numerical analyses of the phenomenon of the workpiece filling the forging die, the resulting die stresses, and the post-deformation heat treatment of the workpiece are being applied increasingly for verification of forging and heat treatment process designs.

2.2 *Material Behavior Constraints and Optimality Criteria*

In addition to dynamic system models, the formulation of an optimal control problem requires a statement of physical constraints and specification of an optimality criterion. The limiting process conditions for acceptable hot workability are important material behavior constraints in the first stage of the control strategy. Here, the acceptable strain rate and temperature variations for hot working metal alloys are based on material flow stability analysis[9] and a desirable and relatively constant apparent activation energy. However, other definitions of safe processing conditions such as those based on Ashby-Frost deformation maps[12] and Raj's damage nucleation maps[13] would also be valid in the optimal control formulation. So, within the acceptable processing variation, a particular thermomechanical trajectory is determined using the prescribed optimality criterion such as producing given hot worked microstructural characteristics. In this article, the problem of microstructure control during dynamic recrystallization is used to illustrate the analysis and optimization technique developed for the first stage of the control strategy. If the microstructural evolution during hot working can be expressed as

$$\text{Grain size} = d(\varepsilon,\dot{\varepsilon},T) \quad [1]$$

and

$$\text{Volume fraction recrystallized} = x(\varepsilon,\dot{\varepsilon},T) \quad [2]$$

and in addition there exists an algebraic relationship between the three material parameters

$$f(\varepsilon,\dot{\varepsilon},T) = 0 \quad [3]$$

then the material behavior of interest can be rewritten as

$$\text{Grain size} = d(\varepsilon,\dot{\varepsilon}) \quad [4]$$

and

$$\text{Volume fraction recrystallized} = x(\varepsilon,\dot{\varepsilon}) \quad [5]$$

Then, an optimality criterion, J, can be set up as

$$J = h\left[\varepsilon(t_f), \dot{\varepsilon}(t_f)\right] + \int_{t_o}^{t_f} g[\varepsilon(t), \dot{\varepsilon}(t)]dt \quad [6]$$

where $h(\cdot,\cdot)$ is the terminal penalty and $g(\cdot,\cdot)$ is the cost over the entire trajectory. The optimality criterion, which is to be minimized to find ε, $\dot{\varepsilon}$, and eventually T via Eq 3, can incorporate a number of physically realistic situations, as is common in standard applications of linear quadratic optimal control. To see this, it is only necessary to define $\varepsilon_{work}(t)$, $\dot{\varepsilon}_{work}(t)$, and $T_{work}(t)$ as nominal trajectories required for material behavior considerations inferred from processing maps and to define $\varepsilon(t)$, $\dot{\varepsilon}(t)$, and $T(t)$ as the actual material parameters to be determined. If it is desired to maintain the material behavior parameters close to those determined from material processing maps, then an appropriate criterion to be minimized could be

$$J_{work} = \int_{t_o}^{t_f} \beta_1(t)\left[\varepsilon(t) - \varepsilon_{work}(t)\right]^2 + \beta_2(t)\left[\dot{\varepsilon}(t) - \dot{\varepsilon}_{work}(t)\right]^2 + \beta_3(t)\left[T(t) - T_{work}(t)\right]^2 dt \quad [7]$$

which when below a certain value ensures that $\varepsilon(t)$, $\dot{\varepsilon}(t)$, and $T(t)$ lie within a family of ellipsoids parameterized by time and reflecting regions of acceptable hot workability properties.

From a microstructural point of view, it also may be desirable to achieve a final grain size, a final fraction recrystallized, and even to maintain the instantaneous grain size below a desired value. Then, an appropriate microstructural optimality criterion would be

$$J_{micro} = \left[x(\varepsilon(t_f), \dot{\varepsilon}(t_f)) - x_f\right]^2 + \left[d(\varepsilon(t_f), \dot{\varepsilon}(t_f))\right]^2 + \int_{t_o}^{t_f} \left[d(\varepsilon(t), \dot{\varepsilon}(t)\right]^2 dt \quad [8]$$

Because it is likely that the two criteria of Eq 7 and 8 will conflict, it is common in control engineering to combine them into a single criterion via weighting constants:

$$J = \alpha_1 J_{work} + \alpha_2 J_{micro} \quad [9]$$

where the relative sizes of α_1 and α_2 are usually obtained from parametric studies on their effect on the material behavior once the minimization of J is carried out. For example, if the microstructural parameters are acceptable but the workability properties are unacceptable for a certain choice of α_1 and α_2, then the penalty on the workability properties may be increased by decreasing α_1 relative to α_2.

The preceding approach to choosing J typically yields an optimality criterion of the form of Eq 6 or more simply

$$J = h(\varepsilon(t_f)) + \int_{t_o}^{t_f} g(\varepsilon(t), \dot{\varepsilon}(t))dt \quad [10]$$

Well-known necessary conditions exist for such an optimality criterion to be a minimum[14] and are partially given by

$$\frac{\partial g}{\partial \varepsilon}(\varepsilon(t), \dot{\varepsilon}(t)) - \frac{d}{dt}\left[\frac{\partial g}{\partial \dot{\varepsilon}}(\varepsilon(t), \dot{\varepsilon}(t))\right] = 0 \quad [11]$$

which generally yields a second-order nonlinear ordinary differential equation. Other necessary conditions depend on the specific boundary conditions, e.g., $\varepsilon(t_f)$ fixed or free, or t_f fixed or free. The necessary conditions taken together lead to a nonlinear two-point boundary value problem, which except in very simple cases must be solved numerically. Also, it is possible that the mathematical form of the functions $g(\cdot,\cdot)$ and $h(\cdot,\cdot)$ in the optimality criterion will be different for different materials. This means that considerable effort may be required simply to set up the two-point boundary value problem. Software based on commercially available symbolic manipulation packages currently is being developed by the authors to automate the problem setup. The resulting two-point boundary value problem can then be approached using standard numerical techniques, the simplest of which is nonlinear shooting.

Once values of $\varepsilon(t)$ and $\dot{\varepsilon}(t)$ are determined that minimize the optimality criterion, $T(t)$ can be determined from Eq 3. This "optimized" thermomechanical trajectory can be viewed as the desired material flow path to be achieved by the process parameters. The next section addresses how process parameters, e.g., ram velocities, can be found to achieve the desired material behavior conditions.

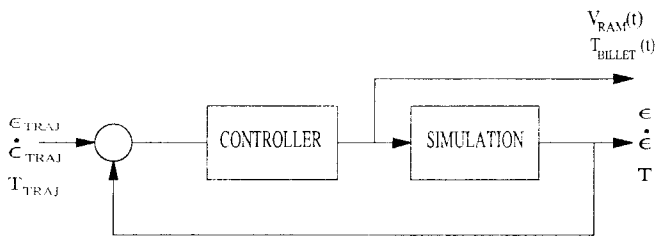

Fig. 2 Block diagram of closed loop control of process simulation.

2.3 *Closed Loop Control of Simulations*

Given a desired set of strain, strain rate, and temperature trajectories, the major difficulty in finding process parameters to achieve the corresponding time varying thermomechanical conditions is the general problem of inhomogeneous deformation and the inability to represent the process in closed form. The approach advocated in this article involves applying closed loop control to process simulations to obtain the desired process parameter trajectories. This concept is illustrated by Fig. 2, where the block labeled "Simulation" is the proper finite-element analysis program such as ALPID for modeling hot deformation processes. The block labeled "Controller" is a possibly nonlinear dynamical system that is designed using standard control system design techniques to ensure that $\varepsilon_{SIM}(t)$, $\dot{\varepsilon}_{SIM}(t)$, and $T_{SIM}(t)$ are at all times close to $\varepsilon_{TRAJ}(t)$, $\dot{\varepsilon}_{TRAJ}(t)$, and $T_{TRAJ}(t)$, i.e., the simulated material behavior "tracks" the desired material behavior. Most importantly, the process parameters $V_{RAM}(t)$ and $T_{BILLET}(t)$, which achieve this tracking in the closed loop, will also achieve the desired trajectories when applied to the simulation alone, as illustrated in Fig. 3. Thus, using closed loop control of the simulation can be viewed as a way to calculate process parameters to achieve desired material behavior and relative uniformity of deformation. If the simulation is sufficiently representative of the actual process, $V_{RAM}(t)$, and $T_{BILLET}(t)$ thus determined can be used as desired control system inputs to be achieved by the processing equipment. It can then be concluded that closed loop control of a process simulation can be used to calculate, in an off-line fashion, control inputs that achieve specified material behavior, uniformity of deformation, and workpiece temperature.

The difficult part of the closed loop simulation approach is designing the controller block in Fig. 2. The problem lies in the fact that the process itself, and hence the simulation, is inherently nonlinear. It is a fact that no completely satisfactory technique exists for designing controllers for such systems. However, a number of approaches to such design problems have been applied successfully for years, most notably in aircraft control over wide variations of altitude, Mach number, and angle of attack. One of the most widely applied such approaches is gain scheduling, in which a different controller (comprised of parameters called "gains" and usually linear) is designed for each of a set of operating conditions. In implementation then, a particular controller is used whenever a certain set

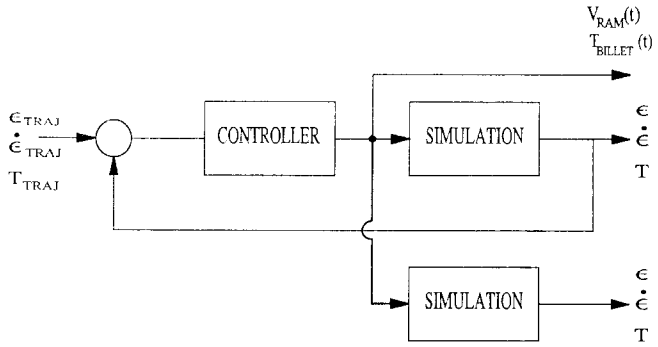

Fig. 3 Illustration of using closed loop process parameter trajectories as open loop controls.

of operating conditions are determined to be in force. The collection of controllers thus designed, along with the algorithm for determining which controller is operating for a given set of operating conditions, is itself a nonlinear controller.

The approach advocated here is a variant of gain scheduling. The underlying assumption is that at various times $t_0, t_1, \ldots, t_N = t_f$, there can be determined corresponding linear system models of the form

$$\dot{x}_k = A_k x_k + B_k \begin{bmatrix} V_{\text{RAM}} \\ T_{\text{BILLET}} \end{bmatrix} \quad [12]$$

$$\begin{bmatrix} \varepsilon \\ \dot{\varepsilon} \\ T \end{bmatrix} = C_k x_k \quad [13]$$

Such models are usually referred to as state-space models, of which much more will be said in Section 3. The important point is that such models can be used to design a sequence of controllers that achieve the material behavior tracking goal. The design of each element of the sequence of controllers is relatively straightforward, and certain techniques for their design lend themselves to a fair amount of automation. For example, once a controller is designed for the linear model at, say, $k = 1$, little or no modification in the controller design parameters is necessary to design a controller for the model valid at $k = 2$. Figure 4 illustrates the concept used for controller design for a particular k. The block labeled "Exo-system" is an unforced, or exogenous, system that is simply a linear model of the desired material behavior trajectory for $t_k \le t < t_{k+1}$, i.e., this block simply generates the inputs for the remainder of the block diagram. The matrix K_k shown in Fig. 4 is designed to minimize

$$J = \int_{t_k}^{t_{k+1}} \left[z_k(t) - z_{k_{\text{TRAJ}}}(t) \right]^T Q \left[z_k(t) - z_{k_{\text{TRAJ}}}(t) \right] + u_k^T(t)\, R u_k(t)\, dt \quad [14]$$

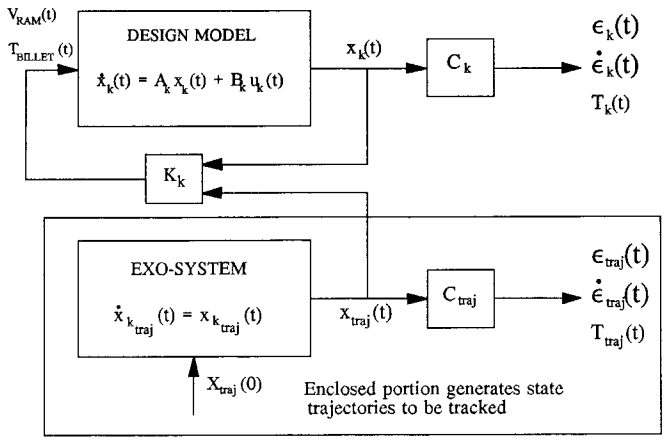

Fig. 4 Block diagram illustrating use of linear models to obtain portions of process parameter trajectories.

where

$$z_k(t) = \begin{bmatrix} \varepsilon_k(t) \\ \dot{\varepsilon}_k(t) \\ T_k(t) \end{bmatrix} \quad [15]$$

$$z_{k_{\text{TRAJ}}}(t) = \begin{bmatrix} \varepsilon_{k_{\text{TRAJ}}}(t) \\ \dot{\varepsilon}_{k_{\text{TRAJ}}}(t) \\ T_{k_{\text{TRAJ}}}(t) \end{bmatrix} \quad [16]$$

and

$$u_k(t) = \begin{bmatrix} V_{k_{\text{RAM}}}(t) \\ T_{k_{\text{RAM}}}(t) \end{bmatrix} \quad [17]$$

where, for example, $\varepsilon_k(t)$ is the portion of $\varepsilon(t)$ over the time interval $t_k \le t < t_{k+1}$. Such a matrix K_k will ensure that the material parameters will track the desired values over the indicated time interval. The matrix weights Q and R usually are chosen to be diagonal matrices with positive elements. The relative sizes of Q and R trade off tracking performance versus the size of the elements of $u_k(t)$.

Although the linear model can be used to calculate the desired $V_{\text{RAM}}(t)$ and $T_{\text{BILLET}}(t)$ over the indicated time interval, it is more accurate to use the higher fidelity finite-element simulation itself to determine these quantities. More important than the accuracy issue, however, is the fact that because $V_{\text{RAM}}(t)$ and $T_{\text{BILLET}}(t)$ over the interval $t_k \le t < t_{k+1}$ affect the simulation and the simulation is nonlinear, the linear model to be used to calculate $V_{\text{RAM}}(t)$ and $T_{\text{BILLET}}(t)$ over the interval $t_{k+1} \le t < t_{k+2}$ cannot be calculated until $V_{\text{RAM}}(t)$ and $T_{\text{BILLET}}(t)$ have been applied as inputs over the interval $t_k \le t < t_{k+1}$. Figure 5 illustrates the results of applying closed loop control to the simulation. This process of sequentially determining $V_{k_{\text{RAM}}}(t)$ and $T_{k_{\text{BILLET}}}(t)$ terminates when it is deter-

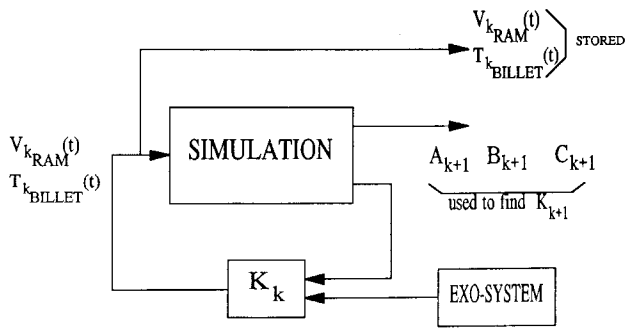

Fig. 5 Illustration of using feedback from linear models to propagate linear models and calculate process parameter trajectories.

mined that the process is complete, e.g., when it is determined that the die is filled.

The technique used here for determining K_k is called the linear quadratic regulator (LQR) methodology in control lexicon. It is often thought of as an optimal control technique because the K_k value determined does indeed minimize a performance criterion as given by Eq 14. However, it should be clearly understood that the resulting $V_{RAM}(t)$ and $T_{BILLET}(t)$ profiles are in no way optimal because the underlying process is nonlinear, a fact not fully taken into account in the calculation. The rationale for choosing LQR as a fundamental part of the scheme for finding the process parameter profiles is (1) the calculation of K_k is done in a straightforward way as the solution of a certain type of matrix equation (the Riccati equation) and (2) once Q and R have been determined that yield an acceptable K_k, it is usually the case that they need not be changed significantly to calculate subsequent values of K. Few other design techniques possess these features, although eigenvalue placement techniques may be able to lend further automation to the design procedure because no choice of Q and R is necessary. A survey of controller design techniques is beyond the scope of this article, but the interested reader can pursue this topic further in Maciejowski.[15]

3. State-Space Modeling

This work uses the systems approach in describing the deformation of material during forging. The material undergoing plastic deformation is conceived as a dynamical system, which maps inputs into outputs through a set of intermediate variables called states. Knowledge of the system states together with the inputs to the system completely describes the behavior of the system. Representing the metalforming system in a state-space form thus facilitates evaluation of the field variables associated with it, and furthermore, by applying a suitable control law, near optimal processing conditions, in terms of the thermomechanical field variables, can also be obtained.

In this work, effective strain rate of the elements of interest and the nodal temperatures of the critical die contacting nodes are taken as the state variables. Because the strain rate is related to the nodal velocities through a gradient matrix, the actual states are the nodal velocities and the nodal temperatures. The input control parameters are the ram velocity and the initial workpiece temperature. Because of the large number of states in the state-space system, order reductions were used for facilitating the control inputs design. Among the available model reduction methods, the balanced model reduction (BMR) approach performed most reliably. Detailed performance comparisons are presented elsewhere.[16]

The finite-element governing equation derived using the variational approach is

$$\mathbf{K}(\mathbf{V})\mathbf{V} = \mathbf{F}(\mathbf{V}) \qquad [18]$$

where $\mathbf{K}$ is the stiffness matrix; $\mathbf{F}$ is the load vector; and $\mathbf{V}$ is the global velocity vector. In Eq 18, $\mathbf{K}$ and $\mathbf{F}$ are functions of $\mathbf{V}$, resulting in a highly nonlinear system of equations. Because of this, the analysis path of the deformation process is traced in an incremental manner by considering a series of discrete equilibrium states, each corresponding to a specific value of time. The velocity distribution at each time step is calculated in an implicit iterative manner until a converged solution is obtained. A Taylor's series expansion is then made about the converged point, resulting in the following linearized system of equations:

$$\mathbf{K}_S\mathbf{V} + \mathbf{K}_T\Delta\mathbf{V} = \mathbf{F} \qquad [19]$$

Here $\mathbf{K}_S$ and $\mathbf{K}_t$ are called the secant stiffness and tangent stiffness matrices, respectively, and are process and material dependent by nature. $\mathbf{K}_S$ and $\mathbf{K}_t$ actually represent the material behavior for the time interval t to $t + \Delta t$.

Finite-element models generally have a large number of degrees of freedom to describe the detailed thermomechanical behavior of the deforming material. A finite-element based-condensation technique is thus devised to eliminate some of the nodal degrees of freedom and retain the critical degrees of freedom. Because the objective is to maintain the desired process conditions in the specified critical regions of the billet, only elements of interest in this region are selected. The nodal degrees of freedom for the elements of interest are retained in the state-space model, whereas those for the rest of the elements are condensed from it by applying suitable boundary conditions. This approach produces a reduced order model that can be used effectively with most control design algorithms. From the linearized mathematical model, the deformation state space form is obtained as[17]

$$\frac{d\mathbf{V}_S}{dt} = \mathbf{A}_D\mathbf{V}_S + \mathbf{B}_D\mathbf{V}_d + \mathbf{W}_D \qquad [20]$$

where $\mathbf{A}_D$ is the plant matrix; $\mathbf{B}_D$ is the input matrix; and $\mathbf{W}_D$ is the constant perturbation vector that results from the condensation process.

Besides deformation analysis, nonisothermal metalforming design requires a thermal analysis to calculate the temperature distribution in the billet and die domains. This thermal analysis involves several separate bodies and the heat transfer between them, because discretization of both the billet and the die must be performed. Finite-element analysis for each body is then considered separately, and the heat transfer between the distinct bodies through the region of contact is modeled by enforcing consistent heat transfer boundary conditions.

The governing heat transfer equation is

$$\mathbf{C}_T\dot{\mathbf{T}} + \mathbf{K}_c\mathbf{T} = \mathbf{Q}_T \qquad [21]$$

where $\mathbf{C}_T$ is the heat capacity matrix, and $\mathbf{K}_c$ is the heat conduction matrix. $\mathbf{Q}_T$ is the heat flux vector that includes the heat generated by plastic deformation, heat radiated between the workpiece and environment, heat convected from the deforming body to the environment, heat conducted across the die/workpiece interface, and heat generated due to friction at the interface. $\mathbf{T}$ is a vector containing the nodal temperatures. To build the thermal state-space model, the above heat flux vec-

tor is linearized in terms of the state variables, namely the nodal velocities and nodal temperatures:

$$\frac{d\mathbf{T}}{dt} = \mathbf{A}_{DT}\mathbf{V} + \mathbf{A}_T\mathbf{T} + \mathbf{B}_{DT}\mathbf{V}_d + \mathbf{H}_d\Delta\mathbf{T}_d + \mathbf{W}_T \quad [22]$$

Here $\mathbf{V}_d$ is the die velocity, and $\Delta\mathbf{T}_d$ is the temperature adjustment. The thermal model also requires condensation similar to the one presented for deformation analysis, to reduce the order of the system. Only the nodal temperatures of the critical die-contacting nodes and the nodal temperatures of the elements of interest are ($\mathbf{T}_I$) are retained, and the reduced order thermal state space representation is obtained as

$$\frac{d\mathbf{T}_I}{dt} = \bar{\mathbf{K}}_{DT}\begin{bmatrix}\mathbf{V}_T\\ \mathbf{V}_I\end{bmatrix} + \bar{\mathbf{K}}_{TP}\mathbf{T}_I + \bar{\mathbf{B}}_{TP}\mathbf{V}_d + \bar{\mathbf{B}}_{TT}\mathbf{T}_d + \bar{\mathbf{W}}_{TP} \quad [23]$$

where $\bar{\mathbf{K}}_{DT}$, $\bar{\mathbf{K}}_{TP}$, $\bar{\mathbf{B}}_{TP}$, and $\bar{\mathbf{B}}_{TT}$ are the condensed matrices, and $\mathbf{W}_{TP}$ is a constant vector resulting from the condensation process. $\mathbf{V}_T$ is the tangential velocity vector at the interfaces, and $\mathbf{V}_I$ is the velocity of critical nodes.

In this study, the effective strain rate of the element of interest is one of the process variables controlled, whereas in Eq 20 and 23 the state variables are the nodal velocities. Therefore, an output equation is used to represent the effective strain rate in terms of the nodal velocities. If the square of the effective strain rate of the element of interest is $\dot{\bar{\varepsilon}}^2$, and $\mathbf{T}_C$ is the output temperature, the output vector y can be formed as

$$y^T = \left[\dot{\bar{\varepsilon}}^2 \mathbf{T}_C^T\right] \quad [24a]$$

The state vector x is given by

$$x^T = \left[\mathbf{V}_T^T \mathbf{V}_I^T \mathbf{T}_C^T\right] = \left[\mathbf{V}_S^T \mathbf{T}_I^T\right] \quad [24b]$$

and the input vector u is given by

$$u^T = [\mathbf{V}_d\ \Delta\mathbf{T}_d] \quad [24c]$$

The above state variables are directly obtained from the computer simulation and finite-element analysis. With the above definitions, a coupled state-space model for a nonisothermal metalforming process is obtained by grouping the deformation state-space model Eq 20 and thermal state space model Eq 23 together as follows:

$$\begin{aligned}\dot{x} &= \mathbf{A}x + \mathbf{B}\mathbf{V}_d + \mathbf{W}_r\\ y &= \mathbf{C}x + \mathbf{E}\end{aligned} \quad [25]$$

Here $\mathbf{A}$ is the plant matrix; $\mathbf{B}$ is the input matrix; $\mathbf{W}$ is a constant vector in $(t, t + \Delta t)$; $\mathbf{C}$ is the output matrix; and $\mathbf{E}$ is a constant vector in $(t, t + \Delta t)$. It should be noted that $\mathbf{W}$ contains certain constant terms coming from the condensation procedure. In retaining these terms, the error between the reduced model and full-size model is greatly reduced, especially in the case of large-scale problems. Compared with the standard state-space models in system theory, Eq 25 can be treated as a system with a constant perturbation $\mathbf{W}_r$. A unique feature of this model is that its dimension keeps changing from step to step because the geometry of the workpiece and boundary condition change with each stroke. The state-space model is thus built and updated at each time step of the simulation. Similarly, reduced order models using the BMR technique are computed at each time step.

4. Preliminary Results

This section presents preliminary results of applying the individual steps of the two-stage method. First, equations describing certain microstructural behavior for plain-carbon steel are used, together with an appropriate optimality criterion, to generate optimal strain and strain rate trajectories for isothermal conditions. The example uses a very simplified description of microstructural evolution and does not represent a fully realistic application of the method of calculating the optimal trajectories; however, it is quite sufficient for serving as a proof-of-concept for the trajectory optimization scheme. Second, a finite-element simulation of a U-section channel forging is used to demonstrate the ability to use closed loop simulations to find process parameter profiles that achieve certain simple requirements on strain rate and temperature.

4.1 *Optimal Trajectory Results*

As an example of the use of this method, simplified versions of the Yada equations[18] for dynamic recrystallization of plain-carbon steel are used to derive optimal trajectories, although the trajectory optimization is expected to be most useful for more challenging materials. The optimality criterion is

$$\mathbf{J} = \int_{t_o}^{t_f} \alpha_1[1 - x(\varepsilon(t))]^2 + \alpha_2\, d^2(\dot{\varepsilon}(t))\, dt \quad [26]$$

where $x(\varepsilon(t))$ is volume fraction recrystallized, and $d(\dot{\varepsilon}(t))$ is dynamic grain size. In this case, the assumed goals are simply to maintain a small grain size and to achieve complete recrystallization. Note that the material behavior constraints are not considered. These quantities are simplified versions of the true Yada equations and are obtained from them by assuming that temperature is constant and the strain for 50% recrystallization is also constant. In the formulation of the Yada equations given in Irwin,[19] the second simplification takes the form

$$\varepsilon_{0.5} = K_4\, d_0^{K_8}\, \dot{\varepsilon}^{K_9} e^{\left(\frac{K_6}{T}\right)} \quad [27]$$

where $\dot{\varepsilon}$ takes the value 1.0 s^{-1} *for this equation only*. This simplification is done simply to make amenable the hand calculation of the required partial derivatives that appear in Eq 11. With these simplifications, the expressions for grain size and fraction recrystallized are, respectively,

$$d(t) = K_{10}[\dot{\varepsilon}(t)]^{K_7} \quad [28]$$

and

$$x(t) = 1 - e^{\left[K_2\left(\frac{\varepsilon-\varepsilon_c}{\varepsilon_{0.5}}\right)^2\right]} \quad [29]$$

where

$$K_{10} = K_1 e^{\left(\frac{QK_7}{RT}\right)} \quad [30]$$

and the remaining constants are

$K_1 = 22{,}600$
$K_2 = -0.693$
$K_4 = 1.144E-3$
$K_6 = 6420$
$K_7 = -0.27$
$K_8 = 0.28$

and

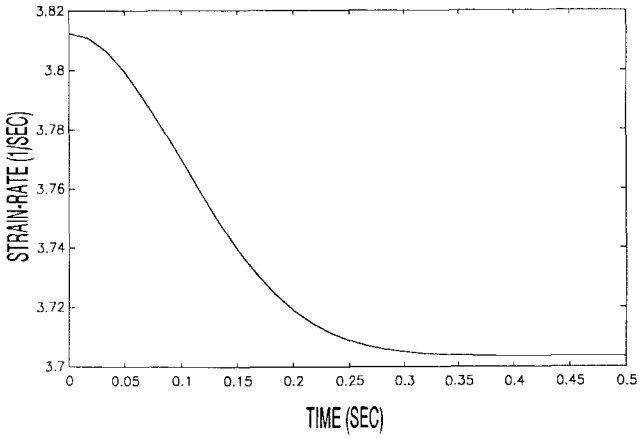

Fig. 6 Optimal strain rate trajectory for microstructure control problem posed for plain-carbon steel.

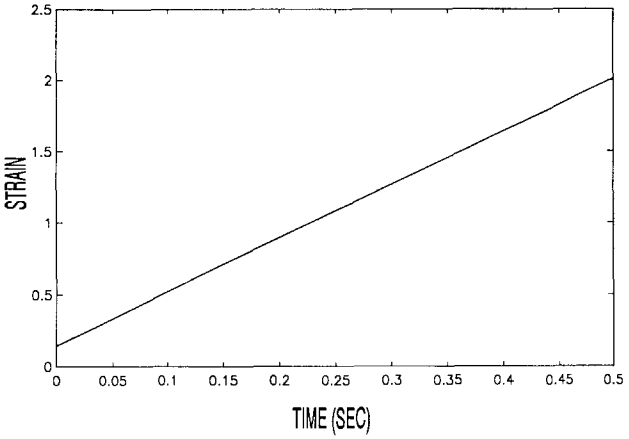

Fig. 7 Optimal strain trajectory for microstructure control problem posed for plain-carbon steel.

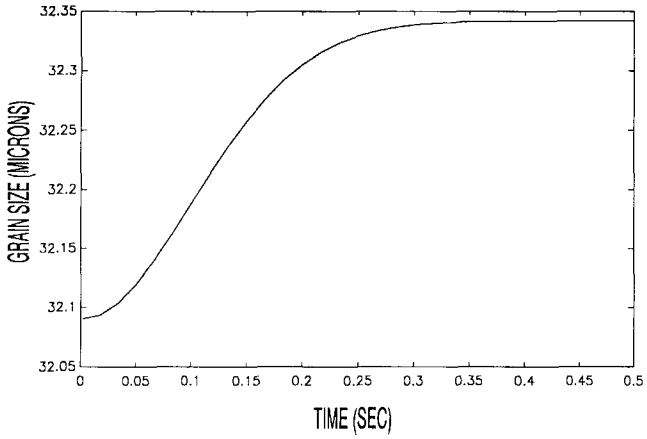

Fig. 8 Predicted grain size behavior from control trajectory found for plain-carbon steel.

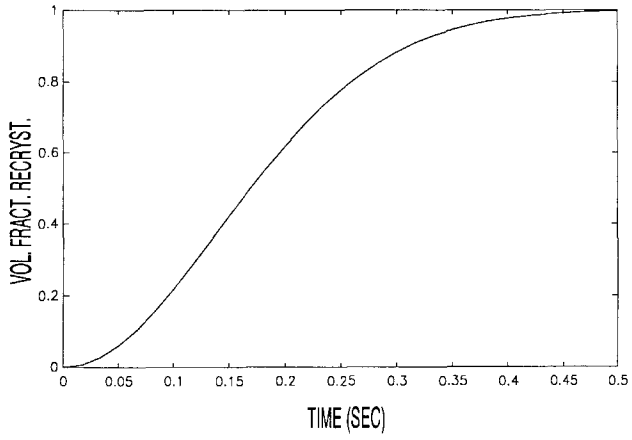

Fig. 9 Predicted fraction recrystallized behavior from control trajectory found for plain-carbon steel.

$K_9 = 0.05$

The numerical results are given in Fig. 6 through 9 for the case in which

$T = 1400$ K

$t_o = 0$

$t_f = 0.5$ s

$\varepsilon(t_o)$ = critical strain + 0.001

$\varepsilon(t_f) = 2$

$\alpha_1 = 25$

and

$\alpha_2 = 1$

Figures 6 and 7 indicate that the optimum strain rate is essentially constant. The strain rate profile in Fig. 6 is shown on an expanded scale to illustrate that the optimization procedure accounts for the fact that microstructural evolution is dynamic in nature and cannot necessarily be treated as a static problem in determining particular values of constant strain rate and constant temperature. The predicted microstructural evolution is shown in Fig. 8 and 9.

The "almost static" situation encountered here is due to the very restrictive assumptions that were necessary to allow the manual derivation of the partial derivatives used in setting up the condition of Eq 11. It is also important to note that workability considerations (again, omitted to obtain a problem amenable to manual derivations of the required partial derivatives) will almost certainly require significant strain rate variations, particularly for more challenging materials. Clearly, a great deal of further investigation of the trajectory optimization technique is needed. These investigations are currently underway using commercially available symbolic manipulation software for automating the derivation of the necessary conditions of Eq 11. However, it is already clear that posing the problem of simultaneously obtaining acceptable microstructural properties and satisfying workability constraints as a dynamic optimization problem is a viable candidate for generating optimal material behavior trajectories.

4.2 *Closed Loop Simulation Results*

In most hot die forging processes, it is desirable to reduce the temperature variation within the deforming workpiece material because it reduces the thermal stresses induced and leads to a more uniform and defect-free microstructural configuration in the final component. The example presented in this sec-

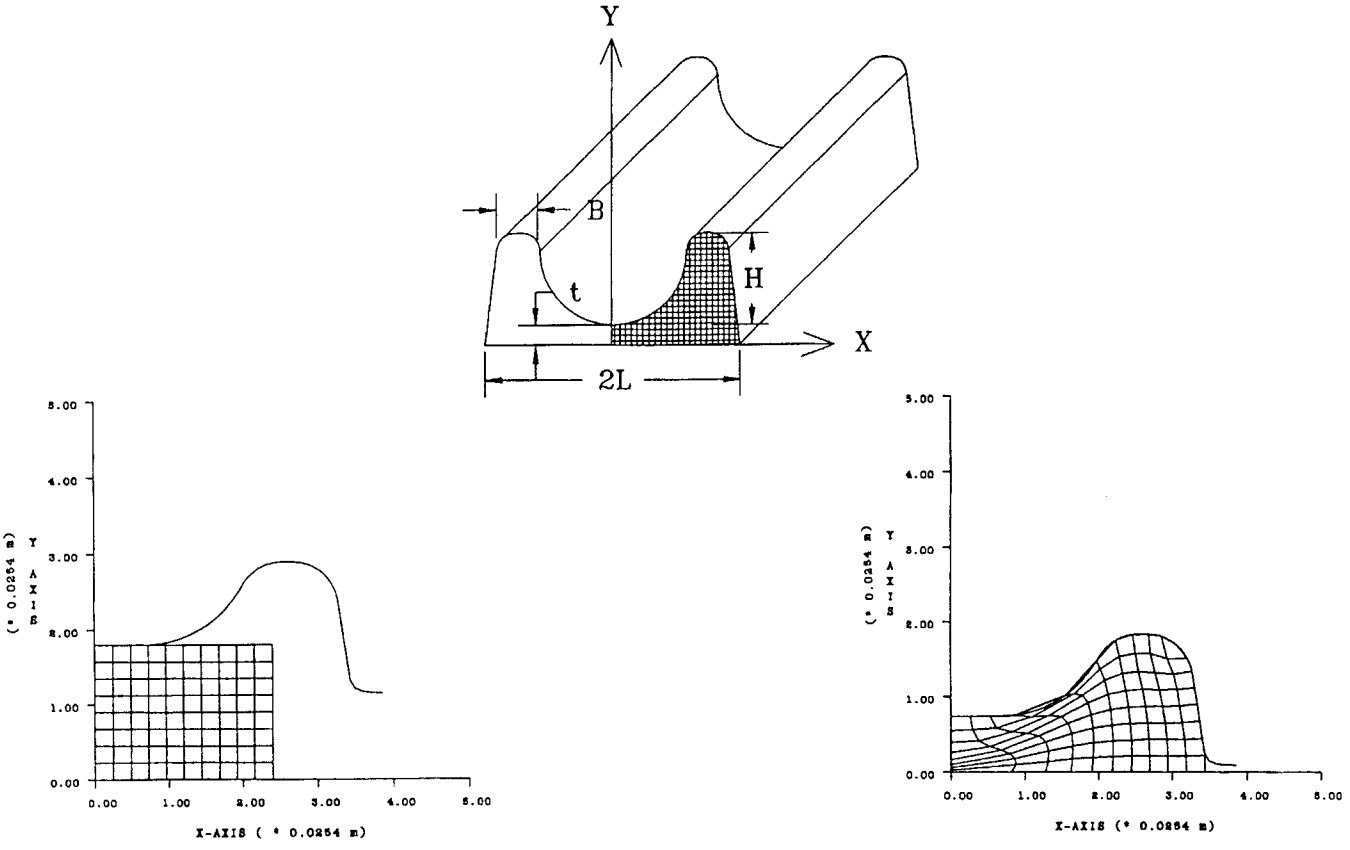

Fig. 10 Finite-element simulation of plane-strain, forging of U-section channel.

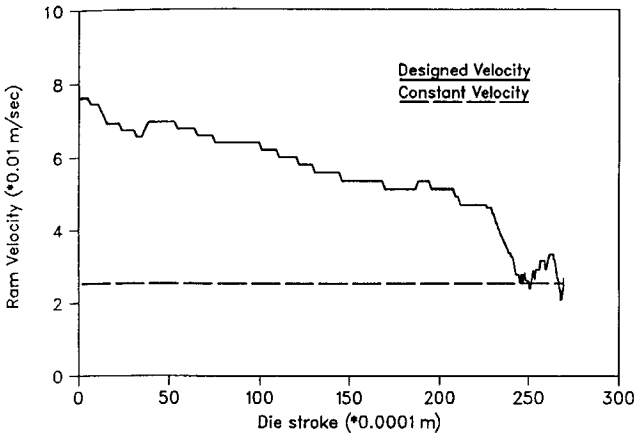

Fig. 11 Comparison of designed and constant die velocity profiles (plane-strain channel section forging).

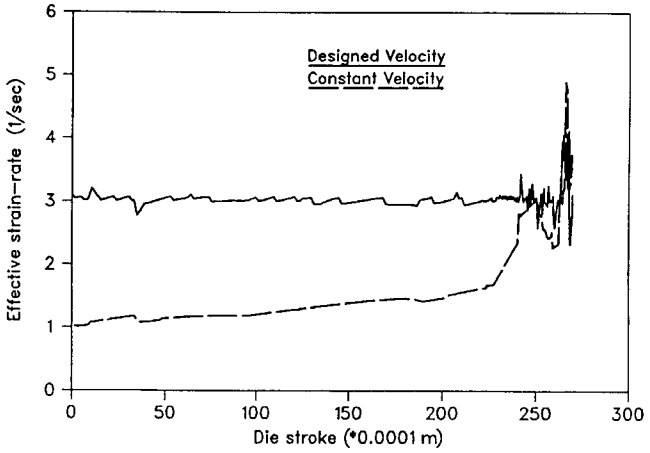

Fig. 12 Maximum effective strain rates in the billet (plane-strain channel section forging).

tion demonstrates how the above objective can be achieved by using the optimal control design scheme developed.

The simulation model used in this example is that of a single-stage, plane-strain, U-section channel forging. Because the channel section is symmetric about the y-axis, only one half of it is modeled and analyzed, as shown in Fig. 10. A rectangular billet made of titanium alloy (Ti-6242) is used as the starting workpiece. The upper die is modeled using 96 elements, and the lower die, which is flat, is modeled with 30 elements. The billet itself is discretized into 80 finite elements. In all cases, four noded isoparametric quadrilateral elements are used for discretization purposes. The frictional condition at the die/workpiece interface is modeled assuming a constant shear friction factor of 0.3. An initial billet temperature of 946 °C and an initial die temperature of 315 °C is assumed at the start of the forging simulation. Simulation is started with an initial die velocity of 7.6×10^{-2} m/s, and the total die stroke needed for completing the forging process is 2.7×10^{-2} m.

The design problem is posed as:

Objective: Reduce the temperature variation in the billet
Subject to: $\dot{\bar{\varepsilon}}_{max} \approx 3.0 s^{-1}$
Design variable: V_d

where V_d is the die velocity; and $\dot{\bar{\varepsilon}}_{max}$ represents the maximum strain rate among all the elements in the deforming material. The constraint is on the rate of deformation and dictates that the maximum effective strain rate in the billet be maintained at 3.0 1/s. The element having the maximum strain rate in the entire workpiece domain can change as deformation progresses. When this occurs, the control scheme automatically selects the new element whose strain rate is to be monitored and controlled. The design variable in this case is the die velocity, which is fed back to the system at every simulation time step to carry out further analysis. The simulation is continued until the specified stroke is reached, and the die is completely filled. The outcome of the entire design procedure is a ram velocity profile that satisfies the design requirement in terms of strain rate and nodal temperature. The processing conditions in this case have been chosen arbitrarily just to demonstrate the methodology. For practical problems, suitable processing conditions may be determined using material processing maps or from the optimal trajectory determined in Stage 1.

Figure 11 depicts the designed die velocity trajectory for this case, whereas Fig. 12 shows the effect of the designed velocity on the strain rate of the deforming material. It may be observed that the maximum strain rate in the workpiece is more or less maintained at the required value. The designed (optimal) ram velocity has an initial value of 7.6×10^{-2} m/s and gradually decreases with progress in deformation, consequently maintaining the strain rate around the required value of 3.0 1/s for the entire process. Toward the end of the stroke, there is a sudden change in deformation mode of the workpiece material as it comes in contact with the far end of the die. As a result, nodes sequentially detach and reattach at the die surface causing some numerical instability in the system model and resulting in some fluctuation in the strain rate (Fig. 12). At the end of the forging process simulation, the lowest temperature in the billet was 795 °C, whereas the highest nodal temperature was 977 °C, thereby resulting in an overall temperature variation of 164 °C throughout the deforming billet.

As a comparative study, the same forging simulation was carried out using a constant ram velocity of 2.5×10^{-2} m/s. From Fig. 12, it is observed that, using this velocity, the maximum effective strain rate approaches the limiting value of 3.0 1/s only at the end of the stroke, whereas it is well below this limit for most of the process. However, a constant die velocity greater than 2.5×10^{-2} m/s would result in very high strain rate values toward the end of the stroke, thereby violating the constraint. This restricts the largest constant velocity that can be used for this process. Because the largest feasible constant die velocity is lower than the designed velocity for almost the entire process, use of the constant velocity results in a higher die/workpiece contact time, allowing for more thermal interaction between the die and the workpiece. This increases the heat lost from the workpiece boundary, giving rise to a large temperature gradient between the boundary and the interior elements of the workpiece. As a result, the temperature range within the billet is also increased. It was determined that, at the

Table 1 Performance of designed process parameters for the U-section channel forging

	Constant velocity	Designed velocity	Change, %
Maximum temperature, °C	973	977	0.40
Minimum temperature, °C	680	795	16.9
Temperature range, °C	275	164	-40.4
Maximum $\dot{\bar{\varepsilon}}$, 1/s	8.5	5.7	-33.0
Minimum $\dot{\bar{\varepsilon}}$, 1/s	0.9	0.6	-33.3
$\dot{\bar{\varepsilon}}$ range, 1/s	7.6	5.0	-34.2
Process time, s	1.0	0.5	-50.0

end of the forging process, the lowest and highest nodal temperatures within the billet, for the constant velocity case, were 680 and 973 °C, respectively, contributing to a temperature range of 275 °C. Using the designed die velocity thus resulted in a 40% reduction in temperature range, thereby satisfying the design objective. The designed velocity also contributed significantly toward reducing the maximum load requirement and overall process time for this forging example. The performance and effectiveness of the design scheme can be gauged from the results tabulated in Table 1.

5. Conclusions and Future Work

A two-stage method of calculating process control parameters for hot metal deformation was presented. The two-stages consisted of (1) calculating optimal strain, strain rate, and temperature trajectories to achieve prescribed material behavior based on process-independent workability and microstructure development models and (2) the use of closed loop control of finite-element-based simulations of the particular metal flow process to calculate process control parameters that achieve the optimal thermomechanical trajectories determined in the first stage. Details of each of the two stages were presented, together with the derivation of the state-space models necessary to the design of closed loop controls for the finite-element simulation. Although the resulting process control parameters approximately achieve the optimal strain, strain rate, and temperature trajectories of the first stage, the parameters themselves are actually only near optimal. Although closed loop control concepts and techniques were used in Stage 2 to calculate the process control parameters, these parameters are open loop inputs to the metalforming process, and the work presented does not represent a closed loop approach to the control of metalforming processes. An independent, simplified example problem for each stage of the current two-stage approach to control system design was presented and solved.

Future work will be directed toward generalizing the optimal trajectory software tools, enhancing the control design techniques used in closed loop simulation control, developing an integrated software environment for calculating process control parameters, and applying the two-stage method to a challenging hot deformation problem, namely forging of gamma titanium aluminide integral blade rotor structures. The immediate goal of all of these enhancements is to enable the verification of the process control strategy in a realistic laboratory environment.

Acknowledgments

This work was conducted as part of the in-house research activities of the Manufacturing Research Branch, Materials Directorate, Wright Laboratory. The authors gratefully acknowledge the assistance of Drs. Venkat Seetharaman and Anil Chaudhary of UES, Inc.

References

1. D.E. Kirk, *Optimal Control Theory: An Introduction*, Prentice-Hall, 1970
2. R.E. Skelton, *Dynamic Systems Control*, John Wiley & Sons, 1988
3. J.J. Jonas, C.M. Sellars, and W.J. McG Tegart, Strength and Structure under Hot Working, *Metall. Rev.*, Vol 14 (No. 1), 1969
4. C.M. Sellars, Recrystallization of Metals During Hot Deformation, *Philos. Trans. Roy. Soc.*, Vol 288 (No. 147), 1978
5. H.J. McQueen and J.J. Jonas, Recovery and Recrystallization During High Temperature Deformation, in *Treatise on Materials Science and Technology, Vol 6, Plastic Deformation of Materials*, Academic Press, 1975, p 393-493
6. W. Roberts, Dynamic Changes That Occur During Hot Working and Their Significance Regarding Microstructural Development and Hot Workability, in *Deformation, Processing, and Structure*, G. Krauss, Ed., ASM International, 1984, p 109-184
7. W. Roberts, Microstructure Evolution and Flow Stress During Hot Working, in *International Conference on Strength of Metals and Alloys*, H.J. McQueen, J.B. Bailon, J.I. Dickson, J.J. Jonas, and M.G. Akben, Ed., Vol 3, Pergamon Press, 1986, p 1859-1891
8. J.C. Malas, "Methodology for Design and Control of Thermomechanical Processes," Ph.D. dissertation, Ohio University, 1991
9. J.C. Malas and V. Seetharaman, Use of Material Behavior Models in the Development of Process Control Strategies, *JOM*, Vol 44 (No. 6), 1992
10. S.C. Jain, Process Modeling and Manufacture: Where We Stand, *JOM*, Vol 41 (No. 2), 1989, p 26
11. S.C. Jain, Emerging Trends in Process Modeling and Manufacture, *JOM*, Vol 42 (No. 2), 1990, p 15
12. H.J. Frost and M.F. Ashby, *Deformation Maps*, Pergamon Press, 1982
13. R. Raj, Development of a Processing Map for Use in Warm-Forming and Hot-Forming Process, *Metall. Trans. A*, Vol 12, 1981, p 1089
14. D.E. Kirk, *Optimal Control Theory: An Introduction*, Prentice Hall, 1970, p 184-209
15. J.M. Maciejowski, *Multivariable Feedback Design*, Addison-Wesley, 1989
16. R.V. Grandhi, R. Thiagarajan, J.C. Malas, and R.D. Irwin, Reduced Order State-Space Models for Control of Metal Forming Processes, *J. Optimal Control Appl. Methods*, 1993
17. R.V. Grandhi, A. Kumar, A. Chaudhary, and J.C. Malas, State Space Representation and Optimal Control of Nonlinear Material Deformation Using the Finite Element Method, *Int. J. Numerical Methods Eng.*, Vol 36 (No. 12), 1993, p 1967-1986
18. C. Devadas, I.V. Samarasekera, and E.B. Hawbolt, The Thermal and Metallurgical State of Steel Strip During Hot Rolling: Part II. Microstructural Evolution, *Metall. Trans. A*, Vol 22, 1991, p 335-348
19. R.D. Irwin, "An Optimal Strategy for Strain, Strain-Rate, and Temperature Trajectories for Dynamic Recrystallization," Final Report, Contract F33615-90-C-5944, Systran, Inc., Sep 1991